25 AUGUST 2003
Volume 83 Number 8

APPLIED PHYSICS LETTERS

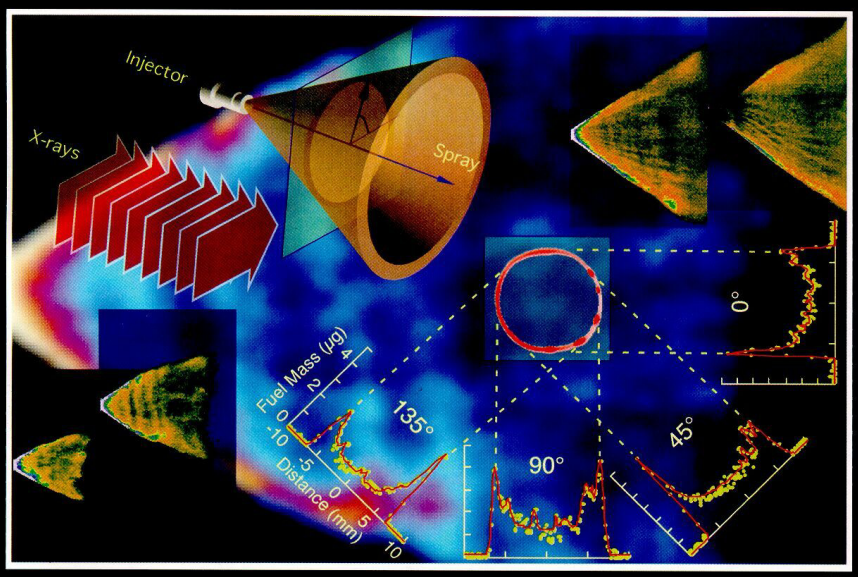

0003-6951(20030825)83:8;1-M

Available online–
See http://ojps.aip.org/aplo/

AMERICAN INSTITUTE OF PHYSICS

Cai, Powell, Yue, Narayanan, Wang, Tate, Renzi, Ercan, Fontes & Gruner. Quantitative analysis of highly transient fuel sprays by time-resolved x-radiography. *Appl. Phys. Lett.* **83** (2003) 1671.

Quantitative analysis of highly transient fuel sprays by time-resolved x-radiography

Wenyi Cai,[a),b)] Christopher F. Powell,[a),c)] Yong Yue,[c)] Suresh Narayanan,[a)] and Jin Wang[a),d)]
Argonne National Laboratory, Argonne, Illinois 60439

Mark W. Tate,[e)] Matthew J. Renzi,[e)] Alper Ercan,[e)] Ernest Fontes,[f)] and Sol M. Gruner[e),f)]
Cornell University, Ithaca, New York 14853

(Received 25 March 2003; accepted 6 June 2003)

Microsecond time-resolved synchrotron x-radiography has been used to elucidate the structure and dynamics of optically turbid, multiphase, direct-injection gasoline fuel sprays. The combination of an ultrafast x-ray framing detector and tomographic analysis allowed three-dimensional reconstruction of the dynamics of the entire 1-ms-long injection cycle. Striking, detailed features were observed, including complex traveling density waves, and unexpected axially asymmetric flows. These results will facilitate realistic computational fluid dynamic simulations of high-pressure sprays and combustion. © *2003 American Institute of Physics.* [DOI: 10.1063/1.1604161]

High-pressure liquid fuel sprays and their atomization and combustion processes are the basis of modern internal combustion engines. Despite decades of intensive experimental and theoretical study,[1] much is still unknown about fuel injection sprays, largely because the fuel aerosols scatter visible light so strongly that the detailed dynamics of fuel and vapor mass distribution cannot be readily imaged. Understanding of the fuel-spray physics is essential for the development of improved engines. For example, recently developed gasoline direct injection (GDI), which injects fuel into the combustion cylinder (as opposed to the air intake port), has greatly improved internal combustion engine performance because of the capability of precise control of the injection rate, timing and combustion of the fuel.[2,3] Quantitative spray characterization has been difficult because it requires microsecond time resolution of submillimeter-scale structures in a complex mixture of liquid and gas. Conventional visible light methods are severely limited by optical multiple scattering from the fuel droplets[4] (see also EPAPS Document #1 for a comparison of visible light shadow graph and x-radiograph of a GDI spray[5]). Other techniques, such as patternators, are capable of probing the near-nozzle region, but perturb the spray and have limited spatial and temporal resolution.[6]

X-radiography is an alternative imaging technique. Recently, we used point-by-point measurement of monochromatic x-ray absorption to quantitatively characterize the dynamics and structure of high-pressure diesel sprays with unprecedented resolution.[8] Point-scanning methods are laborious to image spatially extended gasoline sprays, which are typically a few centimeters across, yet exhibit evolving submillimeter structures. In addition, without two-dimensional imaging capabilities, it is impractical to perform tomographic-type measurements to interrogate the asymmetric and highly transient sprays, which require many images taken from various orientations. In this letter, we report the direct imaging and the quantitative analysis of the GDI hollow-cone sprays by using x-radiography with spatially extended, monochromatic x-ray beams from intense synchrotron x-ray sources and a recently developed fast-framing, two-dimensional x-ray pixel array detector (PAD),[9] at the 1-BM beamline at the Advanced Photon Source (APS) and the D-1 beamline of the Cornell High Energy Synchrotron Source (CHESS).[10]

The prototype commercial GDI injection system tested was designed and fabricated for passenger car applications. A detailed description of the experimental method is given in previous publications[8,10] and in EPAPS Document #2.[5] Figure 1(a) shows a sequence of radiographic images, each 5.1 μs in duration, taken at different instances during the injection: 164 μs, when the spray was just exiting the nozzle; 451 μs, when the spray started to form a stable hollow-cone; 984 μs, when the spray extended to its full range; and 1168 μs, immediately after the nozzle was closed. These images (and, even more dramatically, the radiographic animation consisting of a series of 5.1-μs snapshots taken every 20.5 μs, included as EPAPS Document #3[5]) show striking details in the dynamic characteristics of the hollow-cone gasoline spray. These include a ''sac'' (small volume of fuel near the spray leading edge due to transient nonequilibrium pressures at the instance of the injection pintle lift), density waves (due to a hydrodynamically driven instability in pintle axial motion), heavy asymmetry (due to pintle asymmetric radial motion), and local streaks (due to nozzle surface finish). Each of these features was amazingly reproducible under identical injection conditions. The transmission of monochromatic x-rays through a fuel spray is given by $I/I_0 = \exp(-\mu_M M)$, where I and I_0 are the transmitted and incident x-ray intensities, respectively, μ_M is the mass absorption coefficient of the fuel, and M is the mass of fuel in the beam, given that the absorption variation through the nitrogen gas is negligible.

[a)]Experimental Facilities Division.
[b)]Also at: Naperville Central High School, Naperville, IL 60540.
[c)]Energy System Division.
[d)]Electronic mail: wangj@aps.anl.gov
[e)]Department of Physics.
[f)]Cornell High Energy Synchrotron Source.

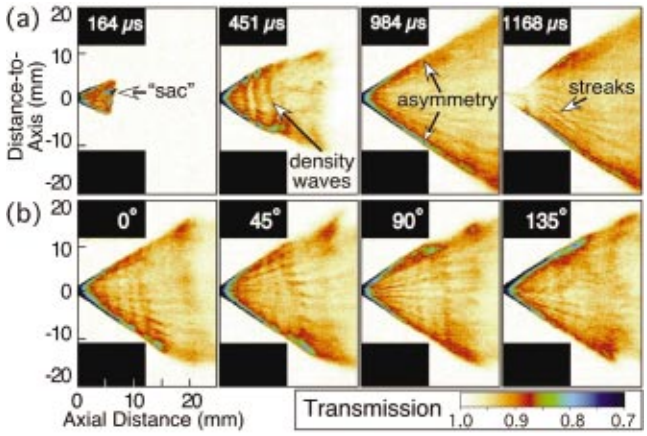

FIG. 1. (Color) X-radiography of hollow-cone direct injection fuel sprays: (a) snapshots of projected fuel mass at various instances, and (b) snapshots taken from four different projection orientations at 1107 μs.

Thus, the time evolution of the measured x-ray transmission I/I_0 can be easily transformed into integrated, line-of-sight fuel mass data at each point in the radiograph. This simple conversion ensures that the mass distribution measurement is quantitative and absolute. The droplet size distribution would not have a noticeable influence on the transmission data.

In order to perform quantitative temporal and spatial analysis of such complex spray characteristics, images from several spray orientations were needed. Tomographic-type x-radiographs, as shown in Fig. 1(b), were collected from four rotational angles (0°, 45°, 90°, and 135°) about the spray axis to facilitate the deconvolution analysis. Again, the progression of the spray is shown in unprecedented detail in the movie of successive frames taken from the four projection directions, as included in EPAPS Document #3.[5] However, it was difficult to apply conventional computed tomographic analysis[11] and density deconvolution and reconstruction methods[12] to the spatially complex and transient sprays viewed from only four orientations; therefore, a model-dependent method was developed to reconstruct the time-resolved fuel distribution. Given that the fuel-density distribution was not homogeneous along either angular or radial directions, two steps of iterative fitting models were

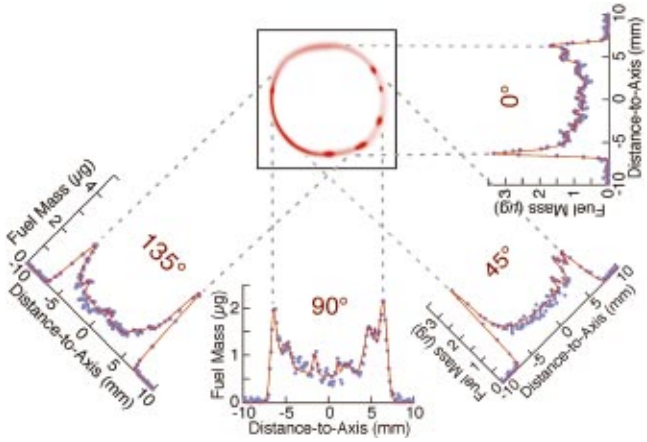

FIG. 2. (Color) Computed fuel mass distribution obtained by fitting the experimental data (circles) with mass deconvolution models (lines) at 820 μs and 8 mm from the nozzle at four projection orientations: 0°, 45°, 90°, and 135°. The fitting procedure is discussed in EPAPS Document #2 (see Ref. 5).

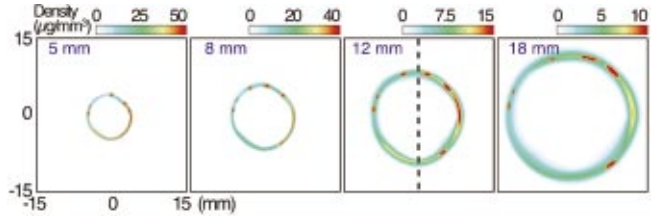

FIG. 3. (Color) Reconstructed fuel density distribution rings at 820 μs with cross-sectioned slices at 5, 8, 12, and 18 mm from the nozzle.

used. First, an asymmetric cone was constructed based on the obvious irregular deviations from symmetry around the spray axis, taking advantage of the multiple images taken at various rotational orientations. Second, details of local structure, in the form of several density peaks, were then added to constitute a more complete model. Finally, the integrated, line-of-sight mass profile of the model in each of four projections was fit to the four transmission curves collectively. The detailed analysis method and reconstruction algorithm are discussed in EPAPS Document #2.[5]

Figure 2 displays a cross section of the fully developed spray cone as obtained from the deconvolution regression. It is apparent that the fuel density and the cone wall width vary around the ring. The greatest difference in density is a factor of 10. The variations in the radius of the ring indicate that the cross section of the spray cone is not perfectly circular. Differences of up to 0.8 mm occurred in the cone wall thickness, showing the strong angular dependence of these parameters. Also present are clear localized peaks with which the reliability of the four deconvolution fits can be verified.

Figure 3 shows the cross-sectional density distribution reconstructed from the calculated matrix at four distances (l=5, 8, 12, and 18 mm) from the nozzle, at 820 μs after the start of injection. The radii of the rings increase farther from the nozzle, corresponding to a well-developed hollow cone even 5 mm from the nozzle. This observation clarifies the confusion about the hollow-cone development based on measurements using visible light techniques, where light scattering near the nozzle precluded inference of an unambiguous conclusion.[7] The averaged diameter ($\overline{r}$) of the hollow cone at each location reveals the true cone angle (full) to be 66.2° at this time instance. The average fuel density is greatest near the cone and falls as the spray progresses outwards. However, the maximum density of 105 μg/mm^3 at only 5 mm from the nozzle is much lower than the liquid density of the test fuel blend (840 μg/mm^3), indicating that the fuel had already undergone atomization. A similar result was found for diesel fuel sprays[8,10] but under much higher injection pressures (typically >50 MPa). The physical existence of the localized density peaks is further substantiated by their con-

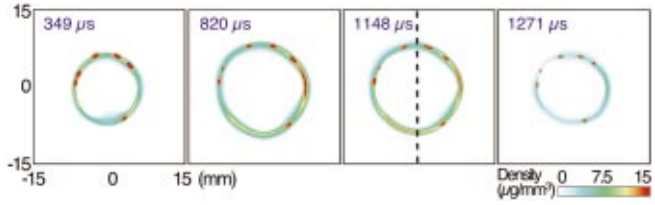

FIG. 4. (Color) Fuel density distribution rings at 12 mm from the nozzle at various instances.

TABLE I. Parameters associated with the fuel distribution at various cross sections of the fuel spray at 820 μs.

l (mm)	$\bar{r}$ (mm)	$\rho_{0_{max}}$ (μg/mm^3)	$\rho_{0_{min}}$ (μg/mm^3)	d_{max} (mm)	d_{min} (mm)	A_M (%)
5	4.45	105	11.7	0.45	0.28	11
8	6.45	55.8	10.1	0.70	0.32	13
12	9.13	74.3	6.37	1.28	0.80	17
18	12.92	69.0	4.78	2.00	1.25	22

stant angular positions in rings at different distances from the nozzle. Parameters from the fitting procedure, including the peak fuel density, ρ_0, show a diverse irregularity and are summarized in Table I, where the spray wall thickness d is defined by $(\sigma_1+\sigma_2)$ (σ_1 and σ_2 are the values of outer and inner Gaussian half-width, respectively, see EPAPS Document #2[5]), and the asymmetry A_M of the distribution is defined as $|M_1-M_2|/(M_1+M_2)$. Here, M_1 and M_2 are the integrated mass values on each side of the ring separated by the dashed line in Fig. 3.

A time series of the cross-sectional fuel density at 12 mm from the nozzle is presented in Fig. 4 at 349 μs, when the spray front just passed the 12-mm mark, 820 μs, when the stable hollow-cone formed; 1148 μs, when the nozzle was closed; and 1271 μs, when the trailing edge of the spray was to arrive at the 12-mm mark. Not only does this show the time development of the hollow-cone average diameter, but the complexity of the spray dynamics is apparent and the asymmetry of the spray persists over the entire injection period. Although the local fuel density distribution varies rapidly, the overall asymmetry shows a large fraction of the total amount of fuel was delivered to a limited solid angle. For example, the amounts of fuel during the injection delivered to the halves separated by the dashed mark in Fig. 4 differ by 55%. This observation indicates that the pintle opened asymmetrically throughout the entire injection process. This asymmetry is more clearly shown in an animation of time evolution of the deconvoluted fuel cross-sectional distribution at 15 mm from the nozzle (EPAPS Document #3).[5] The severe asymmetry may result in uneven combustion and high particulate matter and NO_x emissions since uniform air/fuel mixing cannot be achieved. Spray symmetry is considered a key requirement for GDI engines to reduce fuel droplet size in order to increase fuel dispersion and to facilitate full atomization of the fuel before ignition.[3] The time-resolved, quantitative three-dimensional (3-D) information on the asymmetry and many abnormalities of the sprays revealed in this work, which we have found common to current-generation injectors, may help to explain deficiencies in combustion.

To summarize, the quantitative x-radiographic measurement provides the time-resolved spatial distribution of fuel mass, whether in liquid or vapor form, in a highly transient GDI spray, which has been otherwise difficult to measure in this optically dense near-nozzle region. We also believe that a more comprehensive understanding of the factors affecting the transient fuel density distribution due to fluid instability in the system will enable the development of more realistic and complex fluid-dynamic models of the spray. This is important since experimentation with an actual engine is a lengthy and costly process. To emphasize the generality of this study, the methodology demonstrated here is also suitable to study the fluid dynamics of other high-speed liquid sprays in situations that do not readily lend themselves to analysis by optical methods, such as in dense plasmas, spray coaters, and ink-jet apparatus.

The authors are thankful to R. Poola and R. Sullivan for his initiation of and participation in the research. Technical support from A. G. MacPhee, A. L. McPherson, D. Moran, J. Liu, R. Cuenca, G. E. Geiger, and P. G. VanBrocklin is greatly appreciated. This work and the use of the APS are supported by the U.S. Department of Energy under contract W-31-109-ENG-38. We gratefully acknowledge staff support at the CHESS, funded by the U.S. National Science Foundation (NSF) and the U.S. National Institute of General Medical Sciences via NSF under award DMR-9713424. PAD detector development was funded by DOE grants DE-FG-0297ER14805 and DE-FG-0297ER62443.

[1] *Recent Advances in Spray Combustion: Spray Atomization and Drop Burning Phenomena*, edited by K. K. Kuo (American Institute of Aeronautics and Astronautics, Reston, VA, 1996), Vols. 1 and 2.
[2] D. R. Cohn and J. B. Heywood, Phys. Today **55**, 12 (2002).
[3] F. Zhao, M.-C. Lai, and D. L. Harrington, Prog. Energy Combust. Sci. **25**, 437 (1999).
[4] M. A. Beeck and W. Hentschel, Opt. Lasers Eng. **34**, 101 (2000); V. Sick and B. Stojkovic, Appl. Opt. **40**, 2435 (2001); T. Fujikawa, Y. Hattori, M. Koike, K. Akihama, T. Kobayashi, and S. Matsushita, JSME Int. J., Ser. B **42**, 760 (1999).
[5] See EPAPS Document No. E-APPLAB-83-007334 for comparison between spray images taken by visible light shadowgraphy and x-radiography (#1), description of the experiment and tomographic deconvolution algorithm (#2), images and the progression of the GDI hollow cone spray in the animation of successive frames from 4 measuring angles (#3), and animation of time-evolution of the deconvoluted fuel cross-sectional distribution at 15 mm from the nozzle (#4). A direct link to this document may be found in the online article's HTML reference section. The document may also be reached via the EPAPS homepage (http://www.aip.org/pubservs/epaps.html) or from ftp.aip.org in the directory /epaps/. See the EPAPS homepage for more information.
[6] J. A. Hoffman, J. K. Martin, and S. W. Coates, Rev. Sci. Instrum. **68**, 4247 (1997).
[7] C. S. Lee, K. H. Lee, M. S. Chon, and D. S. Kim, Atomization Sprays **11**, 35 (2001).
[8] C. F. Powell, Y. Yue, R. Poola, and J. Wang, J. Synchrotron Radiat. **7**, 356 (2000).
[9] S. L. Barna, J. A. Shepherd, M. W. Tate, R. L. Wixted, E. F. Eikenberry, and S. M. Gruner, IEEE Trans. Nucl. Sci. **44**, 950 (1997); G. Rossi, M. Renzi, E. F. Eikenberry, M. W. Tate, D. Bilderback, E. Fontes, R. Wixted, S. Barna, and S. M. Gruner, J. Synchrotron Radiat. **6**, 1096 (1999).
[10] A. G. MacPhee, M. W. Tate, C. F. Powell, Y. Yue, M. J. Renzi, A. Ercan, S. Narayanan, E. Fontes, J. Walther, J. Schaller, S. M. Gruner, and J. Wang, Science **295**, 1261 (2002).
[11] L. E. Romans, *Introduction to Computed Tomography* (Williams & Wilkins, Baltimore, 1995); S. R. Stock, Int. Mater. Rev. **44**, 141 (1999).
[12] C. J. Dasch, Appl. Opt. **31**, 1146 (1992); D. C. Hammond, Jr., *ibid.* **20**, 493 (1981).